International Journal of Engineering Trends and Technology
ISSN: 2231-5381/ https://doi.org/10.14445/22315381/IJETT-V73I3P109

Volume 73 Issue 3, 120-129, March 2025

Original Article

Multi-Band Improved Gain Metamaterial Inspired Filtering Antenna Using FDTD Technique for 5G Applications

Sneha Talari[1], Chandra Sekhar Paidimarry[2]

[1,2]*Department of Electronics and Communication Engineering, UCEOU, Telangana, India.*

[1]*Corresponding Author : talarisneha02@gmail.com*

Received: 14 September 2024 Revised: 11 January 2025 Accepted: 17 February 2025 Published: 28 March 2025

Abstract *- In this work, a novel multi-band filtering antenna design and implementation with a Finite Difference Time Domain (FDTD) technique for 5G applications is presented. A hexagonal-shaped microstrip patch antenna is designed with hexagonal metamaterial, which resonates at three different frequencies: 29.835 GHz, 31.282 GHz, and 32.122 GHz. The antenna design takes place on a polyamide substrate with a dielectric constant* ε_r *of 4.3, a loss tangent* $\tan\ \delta$ *of 0.004 and a relative permeability of 1. The novelty of this work is to improve gain by inserting metamaterial into the antenna substrate without increasing antenna size for 5G. The proposed antenna dimensions are* $32.82 \times 25 \times 0.15\ mm^3$*. A Bandpass Filter (BPF) is added to the proposed hexagonal patch antenna elements to select the desired frequency for 5G applications. Finally, the convolutional perfectly matched layer (C-FDTD) technique is used in the proposed antenna model to analyze the electromagnetic fields. We used MATLAB code to implement the FDTD technique and High-Frequency Structure Simulator (HFSS) software to design the antenna. The fabrication of the prototype is done and measured experimentally. The results were in good agreement between simulated, experimental and FDTD. The proposed antenna model can obtain gain values of 6.3 dB, 8.2 dB and 10.2 dB at three resonating frequencies. Its simple, low-profile structure and high gain ensure that the proposed high-gain antenna is well suited for 5G applications.*

Keywords *- 5G applications, Hexagonal patch, Hexagonal metamaterial, Bandpass filter, Finite difference time domain.*

1. Introduction

With the recent advancements in Fifth-Generation (5G) wireless communication systems, there is a growing demand for high-performance antennas operating at high frequencies and providing high gain, wide bandwidth, and low return loss [1],[2]. The high frequencies used in 5G applications, such as 28 GHz and 39 GHz, require antennas with short physical dimensions and high gain to provide sufficient coverage and capacity [3], [4]. Microstrip Patch Antennas (MPA) are well-suited for these applications due to their compact size and high gain. One of the challenges in designing MPA for 5G applications is the control of their frequency response, which is determined by its physical dimensions, the dielectric constant of the substrate, and the thickness of the substrate. To address this challenge, filtering antennas that combine the functions of a filter and an antenna into a single structure have gained significant attention in recent years as they can also reduce the complexity and cost of wireless communication systems [5]. Band-pass filters allow signals within a specific frequency band to pass through while rejecting signals outside the band. Much research is available in the literature, but it has limitations like a lower operating frequency range, an inability to resonate at multiple frequencies, narrow bandwidth, and low gain. Saeed et al. [6] suggested a microstrip patch antenna for 5G applications where slots are etched into the patch, enhancing gain bandwidth and return loss, but failed to achieve miniaturization. Based on a similar design approach, Sowe et al. [7] proposed a patch antenna and achieved gain enhancement by cutting the patch edges, but it altered the resonating frequency. Patel et al. [8] proposed a shaped patch with SRR geometry that exhibited good bandwidth, gain, and radiation pattern performance, but its cost is a drawback. Kiouach et al. [9] designed a band pass filter for 5G mm-Wave where a stepped impedance line stub with a rectangle loop resonator is placed at its centre but has fabrication complexities. Rafal et al. [10] designed a broadband microstrip antenna for 5G wireless systems with high throughput and good bandwidth but with infrastructure limitations. Anurag et al. [11] designed a rectangular patch antenna with double slots that provides good return loss and bandwidth but with a limitation of less efficiency. In order to overcome these existing limitations, a novel multi-band filtering antenna has been designed with the FDTD technique for 5G. In this paper, a multiband filtering microstrip patch antenna for 5G applications has been proposed and analyzed using FDTD and HFSS, followed by an experimental demonstration. To enhance gain, the hexagonal-shaped metamaterial is added to the antenna elements. To enhance the signal transmission and radiation characteristics, a microstrip feed line is inserted into antenna elements and multi-band frequency is achieved by adding a bandpass filter to the antenna elements. The major novelty of this research is obtaining a triple-band filtering patch antenna with hexagonal-shaped metamaterial for enhancing gain and resonating at multiple frequencies simultaneously, representing a significant advancement in multi-band antenna technology, which has been a limitation in existing research and making them suitable for smart cities, IoT and next generation communication systems for efficient future.

2. Materials and Methods

2.1. Design and Structure of Filtering Antenna

This research work presents a novel filtering antenna with FDTD analysis for 5G. The proposed multi-band filtering antenna includes the design of a hexagonal patch antenna with four Hexagonal Split Ring Resonators (HSRR), bandpass filter and microstrip feed line on a polyamide substrate material whose dielectric constant ε_r is 4.3, loss tangent $tan \ \delta$ 0.004 and relative permeability 1. Figure 1 (a-c) represents the proposed filtering hexagonal patch antenna's top view, bottom view and HSRR, and (d-e) represents the fabricated prototype's top view and bottom view. The design of the proposed hexagonal patch antenna is obtained from the base circular patch design.

The four HSRRs are added to the patch and placed on the substrate material to enhance the gain and radiation characteristics of the antenna. Also, HSRR provides excellent electromagnetic properties such as negative permeability and negative permittivity, which can be tailored to achieve desired effects like improved impedance matching and are advantageous in modern communication systems, such as 5G, where compact, efficient, and high-performance antennas are required. The microstrip feed line is added as a feed point, which passes an input impedance of 50 ohms to the antenna design, which enhances the radiation characteristics. It is designed for 5G applications and operates from 28 GHz to 35 GHz. This BPF to the antenna model resonated at three different frequency ranges such as 29.8356 GHz, 31.2822 GHz and 32.1222 GHz. The overall dimension of the antenna is $32.82 \times 25 \times 0.15$ mm^3. Initially, the design of a hexagonal patch is based on a circular structure; the patch antenna's resonating frequency is calculated using the following equation.

$$fre = \frac{Y_{ab}}{2\pi r\sqrt{\varepsilon_r}} C \tag{1}$$

Here Y_{ab} parameter is related to the antenna's geometry, f_{re} represents the patch's resonant frequency, εr is the relative permittivity of a substrate, and c is the velocity of light in free space. The parameter Y_{ab} is obtained using the dimensions of a hexagon-shaped antenna, which can be obtained from the side length of the hexagon. The side of the hexagonal patch antenna (s) is calculated using

$$s = \frac{c}{23.1033 * f\sqrt{\varepsilon_r}} \tag{2}$$

To calculate the radius of the hexagonal patch antenna(r):

$$r = s \times \sqrt{\frac{2.598}{\pi}} \tag{3}$$

Therefore, using equations (2) and (3) in equation (1), the frequency at which the hexagonal patch antenna is resonant is approximated as

$$\mathrm{f_{re}} = \frac{\mathrm{X_{mn}c}}{2\pi s\sqrt{\frac{2.598}{\pi}}.\sqrt{\varepsilon_r}} \tag{4}$$

For TM_{11} mode X_{11}=1.84
For TE_{21} mode X_{21}=3.05

The radius(R) of the circular patch is represented as

$$R = rad\left\{1 - \frac{2M}{\pi r\varepsilon_r}\left(In\frac{\pi r}{2M} + 1.7726\right)\right\}^{1/2} \tag{5}$$

Where M is the height of the substrate and rad is the actual of radius of the patch. The following equation calculates the side length of the inner and outer hexagonal shape.

$$\pi r^2 = \frac{\sqrt[3]{3}}{2} s^2 \tag{6}$$

The physical significance of the suggested model is represented in Table 1.

Table 1. Parameter details for a designed antenna

Specifications	Category
Substrate	Polyamide
Relative permeability	1
Loss tangent	0.004
Dielectric constant	4.3
Length	32.82 mm
Height	25 mm
Width	0.15 mm

The proposed filtering antenna Dimensions are as follows where A=4.92mm, B=2.09mm, C=4mm, D=2.69mm, E=4mm, F=5.87mm, G=4.5mm, H=2.5mm, I=2mm, J=1mm, K=1.5mm, L=0.5mm, M=32.82mm, N=25mm, O=2.5mm, P=1mm, Q=2mm, R=2.25mm, S=2mm, T=1.7mm, U=1.65mm, V=2.25mm and W=0.5mm.

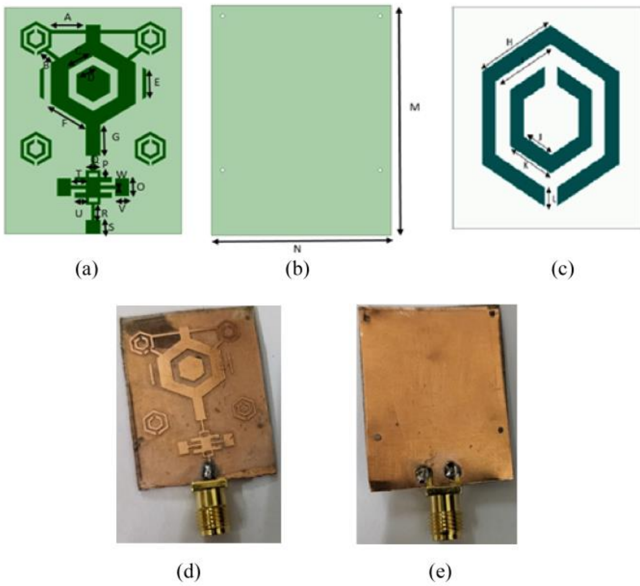

Fig. 1 Proposed filtering antenna (a) Top view (b) Bottom view (c) HSRR (d) fabricated prototype Top view and (e) Bottom view of fabricated prototype

The design procedure of the proposed antenna with metamaterial and the integration of the filter are explained in the following steps, and the design evolution is shown in Figure 2.

Step 1: The hexagonal patch is designed with two slotted ring-based models, and a microstrip feed line is added to the bottom.

Step 2: Two rectangular-shaped strips have been added to the right and left sides of the patch.

Step 3: At the top of the patch, a rectangular slot is added.

Step 4: Four HSRRs have been added to the four sides of the hexagonal patch.

Step 5 and 6: A small strip line is used to connect the HSRR and patch at the top side.

Step 7: Finally, a bandpass filter is added to the feed line of the antenna, and thus, the final proposed filtered antenna is designed.

The experimental prototype has been configured with a separation of 1.5 meters between the transmitter and receiver. The antenna is designed with an Agilent N5247A Vector Network Analyzer (VNA) with firmware version A.09.90.02, which was used to measure antenna scattering parameters (S-parameter). A calibration technique was used to ensure accurate measurements, which helps to minimize systematic errors in VNA in a wider range frequency. Figures 1 (d-e) represent the fabricated antenna prototype's top and bottom views, respectively.

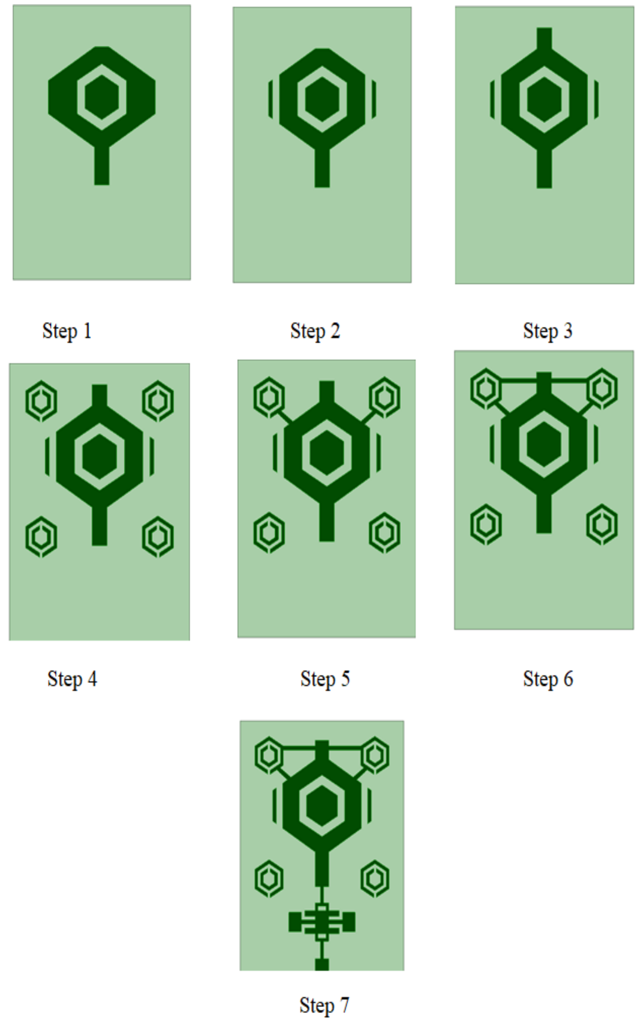

Fig. 2 Design Evolutions of Simulated Antenna Model

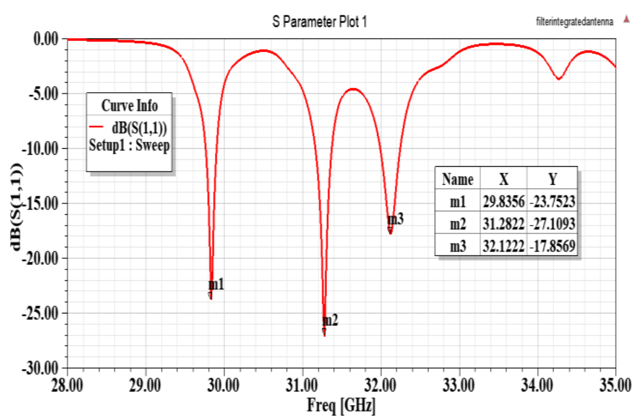

Fig. 3 Return loss (S11) vs frequency of filtering antenna

As depicted in Figure 3, the proposed antenna is resonating at triple band frequencies at 29.835 GHz, 31.282 GHz and 32.122 GHz with return loss values of -23.75 dB,-27.10 dB and -17.85dB, respectively. It is evident that the return loss at triple band frequencies is observed to be less than standard values -15dB, indicating most of the signal power is transferred with low loss, ensuring signal strength with enhanced selectivity, making the antenna more effective in transmitting the required signals while filtering out unwanted frequencies. Thus, the proposed metamaterial-inspired filtering antenna with a return loss of less than -15dB at triple band frequencies provides better efficiency, selectivity, signal clarity and system performance, maintaining a compact design.

2.2. Design of Proposed Band Pass Filter

The bandpass filter design and its equivalent circuit are represented in Figures 4(a) and 4(b). At high frequencies, BPFs are widely used in communication systems because of their ability to select a desired range of frequencies, which is essential when multiple signals are transmitted or received simultaneously. By integrating band pass filters into the design of a patch antenna, it's possible to create a structure that can transmit or receive signals at multiple frequencies while suppressing interference from other frequency bands.

Many structures have been designed in existing research works to obtain high performances of BPF for 5G applications [12]. This existing model has some issues, like high insertion loss. Due to its high speed and convenient wireless access, BPF can obtain high attention in wireless communication and 5G applications. The proposed BPF covers the frequency range from 28 GHz for 5G applications, which is resonated at the frequency range of 31 GHz. This filter has stub-loaded open-loop resonators and Stepped Impedance Resonators (SIR). The filter is designed and simulated on a polyamide substrate whose dielectric constant ε_r=2.2 and thickness h=0.15mm. The filter performance design and optimization are done using HFSS software. In order to make the filter compatible with RF components without any changes, the ground plane is placed on the same substrate. To eliminate spurious response and enhance the stop band performances, rectangular slots are added on both sides of the microstrip in the BPF design. Chebyshev filters of order 6 are used in the design of resonators because of their sharp cut-off characteristics. The slot widths between two low-impedance sections will affect the S-parameters.

The width of the substrate is calculated by using

$$Z_0 = \frac{60}{\sqrt{\varepsilon_{eff}}} log\left(\frac{8h}{w} + \frac{w}{4h}\right) \quad (7)$$

The effective dielectric constant (ε_{eff}) is calculated by using

$$\varepsilon_{\mathrm{eff}} = \frac{\varepsilon_{\mathrm{r}}+1}{2} + \frac{\varepsilon_{\mathrm{r}}-1}{2}\left(1 + 10\frac{\mathrm{h}}{\mathrm{w}}\right)^{-\frac{1}{2}} \quad (8)$$

Thus, changing the width (w) and height (h) in the design can achieve optimized performance.

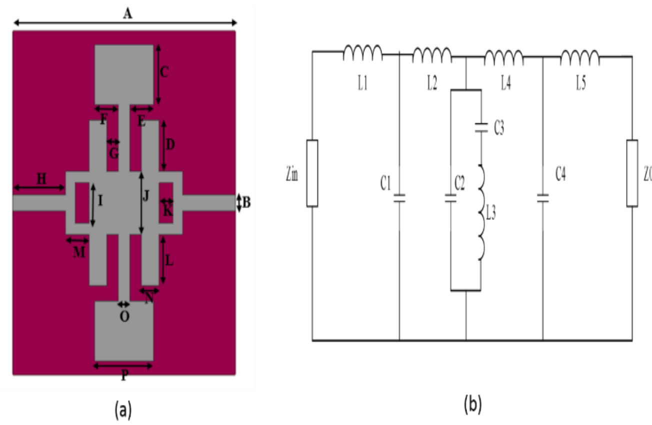

Fig. 4 (a) Band pass filter design, the values are A=9.5mm, B=0.5mm, C=1.9mm, D=1.65mm, E=1mm, F=1mm, G=0.5mm, H=2.25mm, I=1.3mm, J=2mm, K=0.6mm, L=1.65mm, M=1mm, N=0.75mm, O=0.5mm and P=2.5mm, (b)Equivalent circuit of bandpass filter where L1-L5: inductances and C1-C4: capacitances

The dimensions of the designed filter by the HFSS tool are shown in Figure. 4(a). The equivalent circuit model of the BPF filter is represented in Figure. 4(b) consists of a stepped impedance unit and a bandpass response unit. Based on the series ladder network of an inductor (L) and capacitor (C), SIR is modeled in this approach. Figure 5 represents the performance analysis of the reflection coefficient and insertion loss for the filtering design.

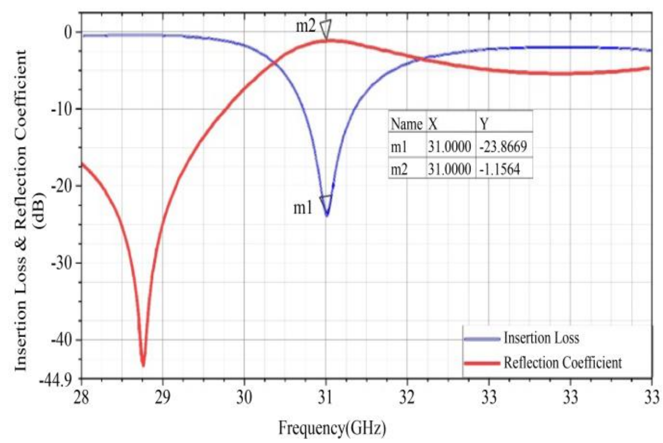

Fig. 5 Performance analysis of filter design: reflection coefficient and insertion loss

As shown in Figure 5, the bandpass filter was analyzed using different performances, such as reflection coefficient and insertion loss. It can obtain values of -23.86 dB at the resonating frequency of 31 GHz for the reflection coefficient and -1.15 dB for insertion loss analysis. Thus, the filter can obtain a reflection coefficient less than the standard value of -15 dB for the operating range of frequency from 28 GHz to 35 GHz. The signal strength has been directly represented by calculating insertion loss. At low insertion loss, the filter can allow more signals to pass through at a certain range of frequencies, which is obtained in this BPF design.

2.3. FDTD Analysis for the Proposed Filtered Antenna

FDTD technique is used to answer simple Maxwell equations [13,14] and calculate the electromagnetic waves 2D of the antenna model based on the simulation parameters. For solving time-dependent Maxwell's equations, Yee [15] proposed a leapfrog arrangement to generate finite difference equations. Controlling the time required for simulation and computer memory usage has been performed using spatial increments$(\Delta a, \Delta b, \Delta c)$, which are related to numerical dispersion error. The mathematical expression of the spatial increments is represented in the following Equation.

$$\Delta t \leq \frac{1}{c\sqrt{\left(\frac{1}{\Delta a}\right)^2+\left(\frac{1}{\Delta b}\right)^2+\left(\frac{1}{\Delta c}\right)^2}} \tag{9}$$

With an increment in spatial dimensions, there is an increase in the numerical dispersion error. This will lead to a reduction in computational time and memory space. Courant-Friedrich-Levy (CFL) stability condition restricts the performance. The magnetic field (H) and electric field (E) based on central difference are updated based on the following equations.

$$\frac{\partial E_a}{\partial t} = \frac{1}{\varepsilon_a}\left(\frac{\partial H_c}{\partial b} - \frac{\partial H_b}{\partial c} - \sigma_a^e E_c - j_{ia}\right) \tag{10}$$

$$\frac{E_a^{m+1}(i,j,k)-E_a^{m}(i,j,k)}{\Delta t} = \frac{1}{\varepsilon_a(i,j,k)} \frac{H_c^{m+\frac{1}{2}}(i,j,k)-H_c^{m+\frac{1}{2}}(i,j-1,k)}{\Delta b} - \frac{1}{\varepsilon_a(i,j,k)} \frac{H_b^{m+\frac{1}{2}}(i,j,k)-H_b^{m+\frac{1}{2}}(i,j-1,k)}{\Delta c} - \frac{\sigma_a^e(i,j,k)}{\varepsilon_a(i,j,k)} E_a^{m+\frac{1}{2}}(i,j,k) - \frac{1}{\varepsilon_a(i,j,k)} j_{ia}^{m+\frac{1}{2}}(i,j,k) \tag{11}$$

$$\frac{\partial H_a}{\partial t} = \frac{1}{\mu_a}\left(\frac{\partial E_b}{\partial c} - \frac{\partial E_c}{\partial b} - \sigma_a^n H_a - M_{ia}\right) \tag{12}$$

$$\frac{H_a^{m+1}(i,j,k)-H_a^{m}(i,j,k)}{\Delta t} = \frac{1}{\mu_a(i,j,k)} \frac{E_b^{m}(i,j,k+1)-H_c^{m}(i,j,k)}{\Delta b} - \frac{1}{\mu_a(i,j,k)} \frac{E_c^{m}(i,j+1,k)-H_b^{m+\frac{1}{2}}(i,j+1,k)}{\Delta b} - \frac{\sigma_a^e(i,j,k)}{\mu_a(i,j,k)} H_a^{m}(i,j,k) - \frac{1}{\mu_a(i,j,k)} M_{ia}^{m}(i,j,k) \tag{13}$$

Here, Perfectly Matched Layers (PML) in a special medium surrounded by a problem space have created wave impedance matching conditions. Convolutional PML conditions are used for the effective absorption of electromagnetic waves. The electromagnetic response of the antenna is evaluated by implementing FDTD equations in the MATLAB platform. Here, the antenna simulated parameters are built into the FDTD model, and the simulation is run to obtain performances like reflection coefficient and radiation patterns. The simulation parameters, resonated frequency ranges, substrate properties, etc, are considered in the first stage. Based on these simulation parameters, the performances are evaluated for FDTD analysis. The simulation time of FDTD has been evaluated by using the following equation.

$$Sim\ FDTD = \frac{2 \times D}{c} \tag{14}$$

Where D is the largest dimension of length, width and thickness and $c = 3 \times 10^8 m/s$, Table 2 represents the simulation parameters for FDTD analysis. Thus, the proposed model has a simulation time of 277ps and a memory size of 207KB. The FDTD model has a grid cell size of $\Delta x, \Delta y, \Delta z = 0.43mm$.

Table 2. FDTD parameters

Parameters	Values
Memory size	207 KB
Simulation time	277 ps
Time step (dt)	0.00089ns

3. Results and Discussions

Several parameters are analyzed to filter the antenna structure and achieve better results for the suggested design. Figure.6 shows the current distribution of the proposed antenna. It represents that a maximum current distribution to the antenna is through the feed line, so have better impedance matching of the antenna and improved radiation characteristics, and minimum current is flowing through HSRR and Stub loaded resonators and symmetrical current distribution in impedance resonators slots and so enhanced the resonance at multiple bands simultaneously.

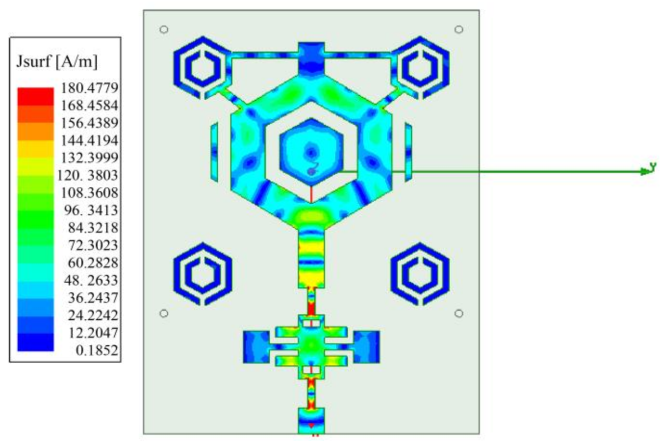

Fig. 6 Surface current density of proposed filtering antenna

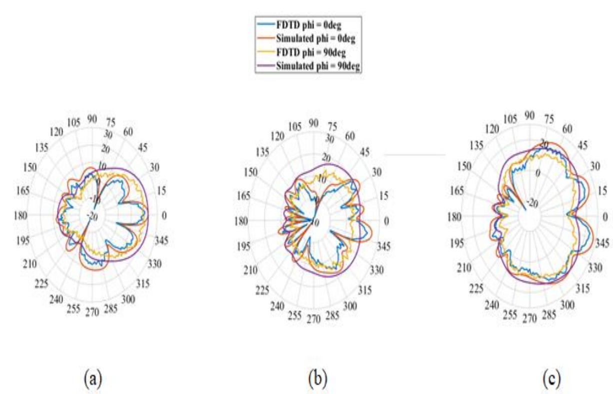

Fig. 7 The radiation pattern for simulated and FDTD at (a) 29.835 GHz, (b) 31.282 GHz, and (c) 32.122 GHz

The comparison analysis of simulated and FDTD radiation patterns is shown in Figure. 7. Here, the main lobe at 0 degrees represents the E-plane, and the sub-lobe at 90 degrees represents the H-plane. At three different resonating frequencies, the proposed antenna can reach values up to a maximum of 20 dB in this analysis for both FDTD and imulated measurements. Achieving up to 20 dB gains a high-performance, reliable and efficient antenna design and can offer excellent versatility across multiple high-performance applications like 5G.

3.1. Gain, Directivity and Radiation Pattern Analysis

Figure 8 depicts the simulated 3D plots of gain, directivity, and radiation pattern for 29.835 GHz, 31.282 GHz and 32.122 GHz, respectively. In this gain analysis, as shown in Figures 8(a-c), the proposed design obtained gain values of 6.3, 8.2, and 10.2 dB, and corresponding directivity values are 9.7, 10.8 and 11.6 dB for 29.835 GHz, 31.282 GHz and 32.122 GHz respectively as shown in Figures 8(d-f).

The gain and diversity plots are used to analyze the diversity performances and show the improvement in signal strength. The strength of the signal is observed linearly with an increase in the frequencies.

The gain plot represents how well the antenna radiates in different directions. Radiation pattern analysis is performed for the antenna model to measure transmitting and receiving electromagnetic waves, which is analyzed in terms of E-plane and H-plane. The antenna's electric and magnetic fields are measured by E and H planes at the direction of 0 degrees and 90 degrees.

Here, the radiation pattern is analyzed in a 3D plot; it can obtain values of 24.1 dB, 26 dB and 27.9dB for the resonating frequency of 29.835 GHz, 31.282 GHz and 32.122 GHz, respectively, as shown in Figures 8(g-i). Here, the exploration of radiation patterns increases with increasing frequency values.

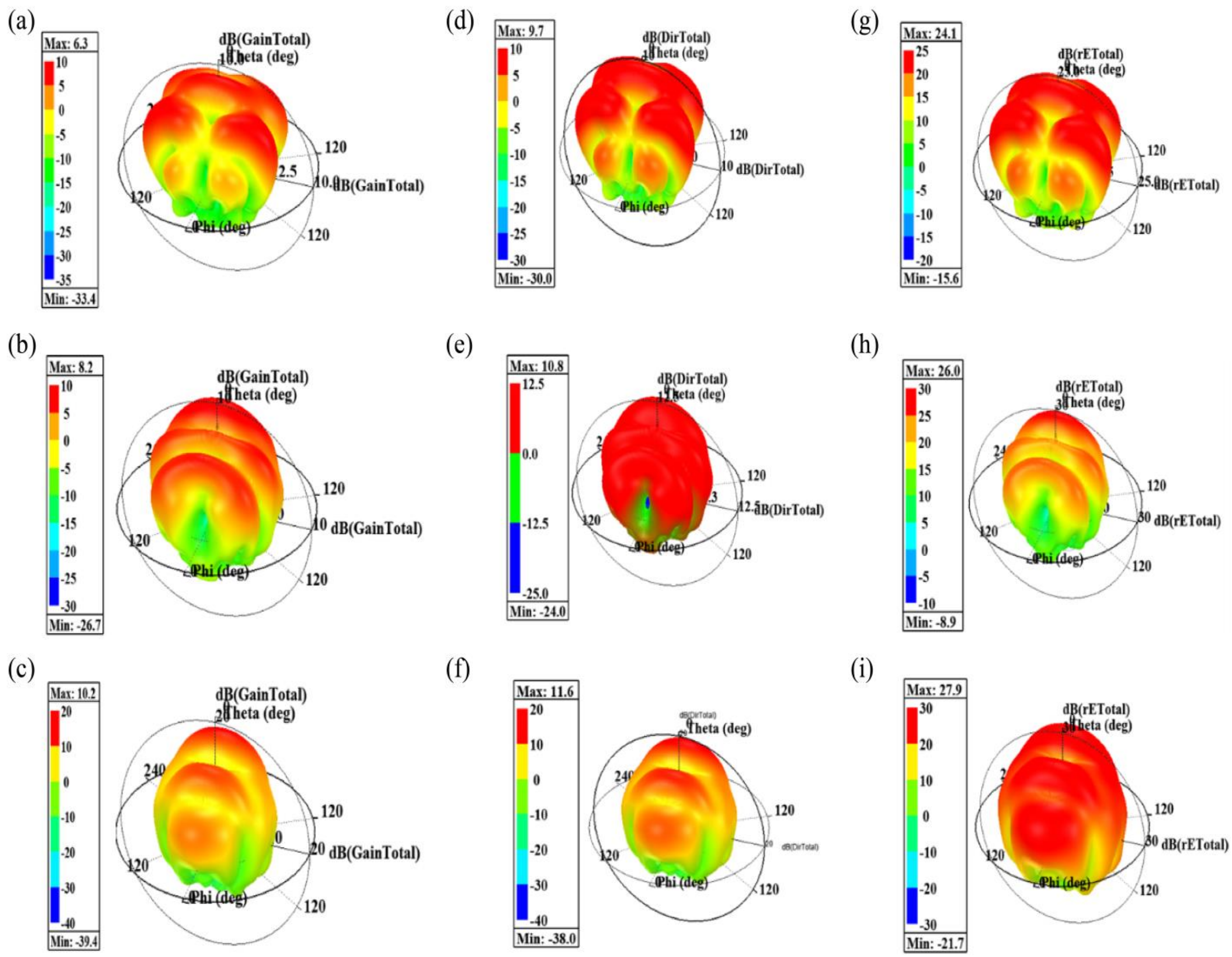

Fig. 8 (a-c) Simulated performance analysis of 3D gain plot, (d-f) 3D directivity plot, (g-i) 3D radiation pattern plot, for (a,d,c) 29.835 GHz, (b,e,h) 31.282 GHz, and (c,f,i) 32.122 GHz, respectively

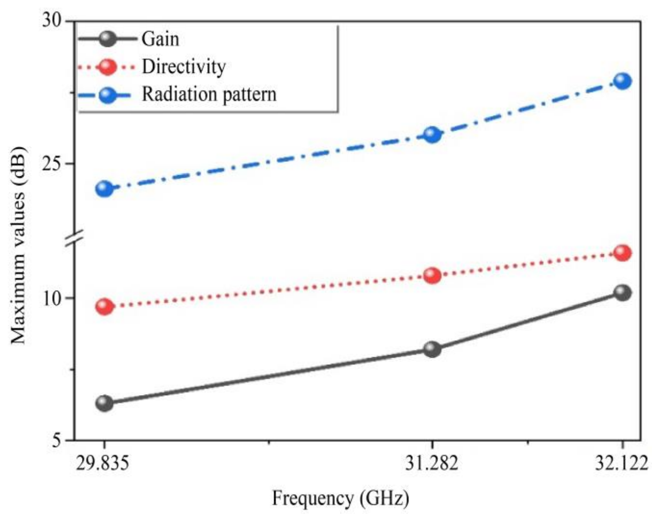

Fig. 9 The maximum values obtained for gain, directivity and radiation pattern from the data shown in Fig. 8

Figure 9 indicates the improvement values obtained for gain, directivity and radiation pattern from the simulated results. At 29.835GHz there obtained a moderate value of gain of 6.3 dB with reasonable efficiency in the radiation of energy and is suitable for shorter-range communication or for applications where broader coverage is needed. At 31.282 GHz, the gain of 8.3 dB means the antenna is focusing energy more effectively, providing better performance and could result in more substantial, more reliable signals over a greater distance.

A gain of 10.2 dB at 32.122GHz indicates a highly efficient antenna. It is used for applications where precise, long-range communication is essential, ensuring minimal power loss and better signal strength in the desired direction. Thus, the increasing gain values across the three frequencies represent the antenna's ability to focus energy more effectively as frequency increases, leading to improved signal strength and efficiency, which is used for high-frequency applications where maintaining strong, directed signals is essential for reliable, high-performance communication.

At 29.835 GHz, the directivity is 9.7 dB. The antenna focuses more energy in the desired direction but still has broader coverage. The increase in directivity, i.e. 10.8 dB at 31.282 GHz, reflects the antenna's ability to focus even more energy toward a specific direction at this higher frequency and is used in applications where slightly more focused energy is needed to overcome interference signals. The directivity of 11.6 dB at 32.122 GHz represents even higher directional focus, making the antenna particularly effective in transmitting energy toward a narrow beam and is helpful for long-range, high-frequency communication.

The radiation pattern values of 24.1 dB, 26 dB, and 27.9 dB at the respective frequencies show a progressive increase in directionality. As frequency increases, the antenna's radiation becomes more focused in the desired direction. This progression represents that the antenna’s improved performance at higher frequencies is used for high-frequency, high-precision applications.

The proposed antenna is analyzed using various performance methods, such as simulation-based analysis, measured analysis, and FDTD analysis. From this overall analysis, the simulated, measured, and FDTD resonating frequencies are within the agreement of the frequency range of 5G, representing the antenna's better performance in signal transmission and communication speed when used for 5G.

Table 3 represents the performance analysis for various existing and proposed antenna models. It is observed that the proposed antenna has better performance than other existing research. This approach can obtain high gain, multiple bands and a high range of resonating frequencies.

Table 3. Summary of a few of earlier designed antenna comparisons with our results

Antenna size (mm^3)	Operating Frequency (GHz)	Substrate	Antenna model	Gain (dB)	Reflection coefficient (dB)	Band	Ref
$32 \times 32 \times 0.8$	2 GHz– 30 GHz	FR-4 epoxy	Patch antenna	3.3	<-20	Dual	[6]
$9.7 \times 9.9 \times 0.508$	More than 28 GHz	Rogers RT 5880	Slotted patch	>5.4	<-21.5	Dual	[20]
$5.959 \times 5.959 \times 1.4$	22 GHz-34 GHz	FR-4	Circular patch	0.1573	<-23	Single	[21]
$35 \times 39 \times 1.57$	28 GHz to 30 GHz	Teflon	Rectangular patch	>6.1	<-20	Single	[22]
$\mathbf{32.82 \times 25 \times 0.15}$	**28 GHz to 35 GHz**	**Polyamide**	**Filtering antenna with FDTD**	**6.3 8.2 10.2**	**< -25**	**Triple**	**In this Work**

3.2. Return Loss: Comparison between Simulated, FDTD and Experimental Measurements

The return loss (reflection coefficient) for a proposed antenna with a bandpass filter from the simulation, FDTD and experimentally measured values are evaluated in Figure 10 (a). The Simulated resonating frequencies were obtained at 29.8356 GHz, 31.2822 GHz and 32.122 GHz and for FDTD, there is a smaller frequency shift compared to simulation results followed by 29.54 GHz, 31.00 GHz and 31.82 GHz, respectively. However, the experimentally obtained resonant frequencies lie between the Simulated and FDTD values. For instance, the measured frequencies are 29.79GHz, 31.17GHz and 32.20GHz. The performance comparison for the proposed filtering antenna in simulation, measured, and FDTD analysis is in Table 4. The obtained return loss values for simulated, measured, and FDTD values of the antenna obtained are of -23.7523 dB, -27.1093 dB and -17.8569 dB at 29.8356 GHz, 31.2822 GHz and 32.122 GHz, -17.86dB, -19.83dB, -13.89dB at 29.79GHz, 31.17GHz and 32.20GHz and -19.28dB, -22.512 dB and -17.205 dB at the resonating frequency of 29.54 GHz, 31.00 GHz and 31.82 GHz.

The measured values are evaluated when the suggested antenna is fabricated in real time. As can be seen, the simulated, measured, and FDTD results are in reasonable agreement with frequency bands operating between 28 GHz and 35 GHz, which can be used for 5G applications. FDTD analysis is performed for the proposed model based on simulation parameters. The Voltage Standing Wave Ratio (VSWR) analysis of simulated and measured are evaluated in Figure 10(b).

The proposed antenna model can obtain VSWR values of 1.16, 1.10 and 1.30 for the resonating frequency of 29.83 GHz, 31.28 GHz and 32.12 GHz for simulation analysis and the measured values of VSWR of 2.14, 1.09 and 2.98 at a resonating frequency of 29.79 GHz, 31.17GHz and 32.20GHz. Thus, the performance evaluation in simulation, measured, and FDTD results ensures that the proposed antenna achieved a good VSWR and low return loss at triple band frequencies, indicating that it can be used in advanced communication systems requiring high efficiency and low interference used for 5G.

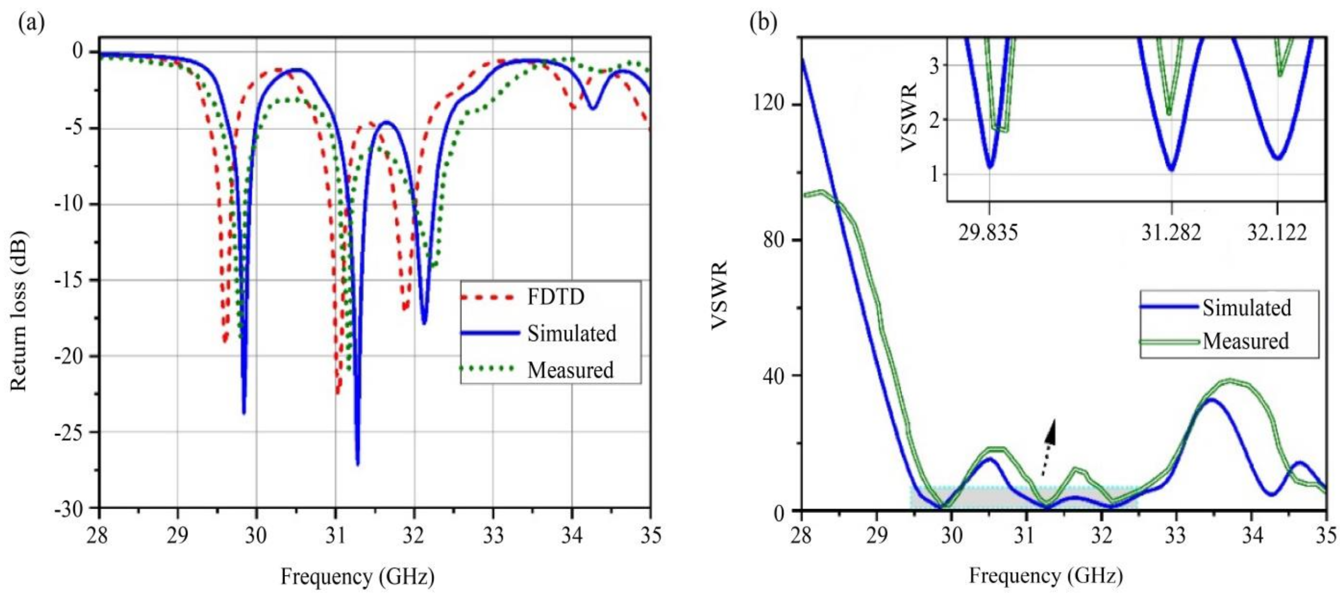

Fig. 10 (a) Simulated, Measured, and FDTD return loss (S_{11}), and (b) Simulated, Measured VSWR measurements

Table 4. Performance analysis of filtering antenna

Analysis	Resonating Frequency (GHz)	Reflection coefficient (dB)	VSWR	Band	Operating Frequency Range (GHz)
Simulation	29.8356 31.2822 32.122	-23.7523 -27.1093 -17.8569	1.16 1.10 1.30	Triple	28-35
Measured	29.79 31.17 32.20	-17.86 -19.83 -13.89	2.14 1.09 2.98	Triple	28-35
FDTD	29.54 31.00 31.82	-19.2878 -22.512 -17.205	-	Triple	28-35

From simulated, measured, and FDTD results, the frequency around 29 GHz is used for satellite uplinks in the k_a band (26.5 GHz-40 GHz) to enable satellite TV services and satellite internet and in 5G networks to provide high-speed connectivity for supporting high bandwidth and low latency communication. The frequency around 31GHz is used for providing high-speed internet and telecommunication systems in fixed wireless access. The frequency of around 32 GHz is used in millimeter wave radar applications, defense and military applications. Therefore, the resonated triple band frequencies obtained for the proposed filtering antenna support various applications, particularly in the emerging 5G and beyond infrastructure.

4. Conclusion

This work proposes a novel bandpass filter-based metamaterial-inspired hexagonal-shaped patch antenna for 5G applications. The antenna dimensions are 32.82 X 25 X 0.15 mm^3. Here, the hexagonal-shaped metamaterial enhances the gain between the antenna model. The BPF simultaneously resonates at different frequencies and reduces the noise in the resonating bands. The proposed antenna model is analyzed using various performances such as reflection coefficient, VSWR, gain, directivity, radiation pattern, etc. The prototype of the filtering antenna is manufactured, and its performance, like resonating frequencies, return loss and VSWR, is measured. The measured and FDTD results are compared with simulation results, and it was found that they operate in the frequency range from 28GHz to 35GHz for 5G applications. Here Convolutional FDTD is used by leveraging the fast convolutional operations, reducing both memory requirements and computational complexity. The results showed that the filtering antenna has peak Gain values of 6.3 dB, 8.2 dB and 10.2 dB at three different resonating frequencies. Thus, the proposed antenna achieved higher gain, compact size, and superior interference suppression than state-of-the-art techniques. In future, the proposed antenna model in this work could be improved by adding multiple ports to enhance the real-time performance.

Acknowledgements

The authors thank the University College of Engineering, Osmania University, for the technical support and experimental support provided by IIT Roorkee.

Data Availability Statement

The data that support the findings of this study are available on request from the corresponding author.

References

[1] M. Kamran Shereen, M.I. Khattak, and Jamel Nebhen, “A Review of Achieving Frequency Reconfiguration through Switching in Microstrip Patch Antennas for Future 5G Applications,” *Alexandria Engineering Journal*, vol. 61, no. 1, pp. 29-40, 2022. [CrossRef] [Google Scholar] [Publisher Link]

[2] Lijaddis Getnet Ayalew, and Fanuel Melak Asmare, “Design and Optimization of PI-Slotted Dual-Band Rectangular Microstrip Patch Antenna Using Surface Response Methodology for 5G Applications,” *Heliyon*, vol. 8, no. 12, pp. 1-14, 2022. [CrossRef] [Google Scholar] [Publisher Link]

[3] Rishitha Kyama et al., “Design and Analysis of Microstrip Rectangular Patch Antenna for 5G Applications,” *4th International Conference on Design and Manufacturing Aspects for Sustainable Energy*, vol. 391, pp. 1-9, 2023. [CrossRef] [Google Scholar] [Publisher Link]

[4] John Colaco, and Rajesh Lohani, “Design and Implementation of Microstrip Patch Antenna for 5G Applications,” *5th International Conference on Communication and Electronics Systems*, Coimbatore, India, pp. 682-685, 2020. [CrossRef] [Google Scholar] [Publisher Link]

[5] Ningning Yan, Hetian Zhou, and Kaixue Ma, “A Filtering Antenna with Slots and Stacked Patch Based on SISL for 5G Communications,” *Electronics*, vol. 12, no. 6, pp. 1-12, 2023. [CrossRef] [Google Scholar] [Publisher Link]

[6] Noor Haider Saeed, Malik Jasim Farhan, and Ali Al-Sherbaz, “Design and Analysis of Microstrip Antenna for 5G Applications,” *Journal of Engineering and Sustainable Development*, vol. 28, no. 2, pp. 285-293, 2024. [CrossRef] [Google Scholar] [Publisher Link]

[7] Mbye Sowe, Dominic BO Konditi, and Philip K. Langat, “A Compact High-Gain Microstrip Patch Antenna with Improved Bandwidth for 5G Applications,” *International Journal of Electrical and Electronics Research*, vol. 10, no. 2, pp. 196-201, 2022. [CrossRef] [Google Scholar] [Publisher Link]

[8] Upesh Patel et al., “Split Ring Resonator Geometry Inspired Crossed Flower Shaped Fractal Antenna for Satellite and 5G Communication Applications,” *Results in Engineering*, vol. 22, 2024. [CrossRef] [Google Scholar] [Publisher Link]

[9] Fatima Kiouach, Bilal Aghoutane, and Mohammed El Ghzaoui, “Novel Microstrip Bandpass Filter for 5G mm-Wave Wireless Communications,” *E-Prime-Advances in Electrical Engineering, Electronics and Energy*, vol. 6, pp. 1-6, 2023. [CrossRef] [Google Scholar] [Publisher Link]

[10] Rafal Przesmycki, Marek Bugaj, and Leszek Nowosielski, “Broadband Microstrip Antenna for 5G Wireless Systems Operating at 28GHz,” *Electronics*, vol. 10, no. 1, pp. 1-19, 2021. [CrossRef] [Google Scholar] [Publisher Link]

[11] Anurag Nayak, Shreya Dutta, and Sudip Mandal, “Design of Dual Band Microstrip Patch Antenna for 5G Communication Operating at 28 GHz and 46 GHz,” *International Journal of Wireless and Microwave Technologies*, vol. 13, no. 2, pp. 43-52, 2023. [CrossRef] [Google Scholar] [Publisher Link]

[12] Thierno Amadou Mouctar Balde, Franklin Manene, and Franck Moukanda Mbango, “A Dualband Bandpass Filter with Tunable Bandwidths for Automotive Radar and 5g Millimeter-Wave Applications,” *Indonesian Journal of Electrical Engineering and Computer Science*, vol. 27, no. 1, pp. 309-317, 2022. [CrossRef] [Google Scholar] [Publisher Link]

[13] Allen Taflove, and Susan C. Hagness, *Computational Electrodynamics: The Finite-Difference Time-Domain Method*, The Electrical Engineering Handbook, Elsevier Academic Press, pp. 1-1006, 2005. [Google Scholar] [Publisher Link]

[14] Yang Hao, and Raj Mittra, *FDTD Modeling of Metamaterials: Theory and Applications*, Artech House, London, pp. 1-380, 2008. [Google Scholar] [Publisher Link]

[15] Kane Yee, “Numerical Solution of Initial Boundary Value Problems Involving Maxwell’s Equations in Isotropic Media,” *IEEE Transactions on Antennas and Propagation*, vol. 14, no. 3, pp. 302-307, 1966. [CrossRef] [Google Scholar] [Publisher Link]

[16] Hesham Mahmoud Emara et al., “Compact High Gain Microstrip Array Antenna using DGS Structure for 5G Applications,” *Progress in Electromagnetics Research C*, vol. 130, pp. 213-225, 2023. [CrossRef] [Google Scholar] [Publisher Link]

[17] Quanwei Wu, Yan Shi, and Long Li, “Wideband Dual-Polarized Differential-Fed Filtering Microstrip Patch Antenna with High Suppression and Wide Stopband,” *International Journal of RF and Microwave Computer-Aided Engineering*, vol. 2023, no. 1, pp. 1-10, 2023. [CrossRef] [Google Scholar] [Publisher Link]

[18] Akinwale O. Fadamiro et al., “Design of a Multiband Hexagonal Patch Antenna for Wireless Communication Systems,” *IETE Journal of Research*, vol. 68, no. 3, pp. 1675-1682, 2022. [CrossRef] [Google Scholar] [Publisher Link]

[19] Thierno Amadou Mouctar Balde, Franklin Manene, and Franck Moukanda Mbango, “A Dualband Bandpass Filter with Tunable Bandwidths for Automotive Radar and 5G Millimeter-Wave Applications,” *Indonesian Journal of Electrical Engineering and Computer Science*, vol. 27, no. 1, pp. 309-317, 2022. [CrossRef] [Google Scholar] [Publisher Link]

[20] Mouaaz Nahas, “A Super High Gain l-Slotted Microstrip Patch Antenna for 5G Mobile Systems Operating at 26 and 28 GHz,” *Engineering, Technology & Applied Science Research*, vol. 12, no. 1, pp. 8053-8057, 2022. [CrossRef] [Google Scholar] [Publisher Link]

[21] Awatef Djouimaa, and Karima Bencherif, “Design of a Compact Circular Microstrip Patch Antenna for 5G Applications,” *Engineering, Technology & Applied Science Research*, vol. 14, no. 4, pp. 16020-16024, 2024. [CrossRef] [Google Scholar] [Publisher Link]

[22] Md. Jasim Uddin Qureshi et al., “Design and Performance Analysis of a Broadband Rectengular Microstrip Patch Antenna for 5G Application,” *2023 2nd International Conference on Paradigm Shifts in Communications Embedded Systems, Machine Learning and Signal Processing (PCEMS)*, Nagpur, India, pp. 1-6, 2023. [CrossRef] [Google Scholar] [Publisher Link]